AD8620ARZ-HX Precision, Very Low Noise,Low Input Bias Current, Wide Bandwidth JFET Operational Amplifiers

Description

The AD8620ARZ-HX is a high-precision JFET input amplifier that features an ultra-low offset voltage and drift, minimal input voltage and current noise, very low input bias current, and a wide bandwidth. Unlike many other JFET amplifiers, the AD8620ARZ-HX maintains a low input bias current across the entire operating temperature range. This amplifier is stable with capacitive loads exceeding 1000 pF in non-inverting unity gain configurations; significantly larger capacitive loads can be driven effortlessly at higher noise gains. The output of the AD8620ARZ-HX can swing to within 1.2 V of the supply rails even under a 1 kΩ load, thereby maximizing dynamic range even when supply voltages are limited. The outputs exhibit a slew rate of 50 V/μs in both inverting and non-inverting gain configurations and achieve settling to 0.01% accuracy in less than 600 ns. With its high input impedance, exceptional precision, and substantial output drive capability, the AD8620ARZ-HX is ideally suited for driving high-performance ADC inputs as well as buffering DAC converter outputs.

Applications for the AD8620ARZ-HX encompass electronic instruments; ATE amplification; buffering and integrator circuits; CAT/MRI/ultrasound medical instrumentation; instrumentation-quality photodiode amplification; fast precision filters (including PLL filters); and high-fidelity audio systems.

The AD8620ARZ-HX is fully specified over an extended industrial temperature range of −40°C to +125°C. It is available in a narrow 8-lead SOIC package.

Features

- Low noise: 6 nV/√Hz
- Low offset voltage: 100 μV maximum
- Low input bias current: 10 pA maximum
- Fast settling: 600 ns to 0.01%
- Low distortion
- Unity gain stable No phase reversal
- Dual-supply operation: ±5 V to ±13 V

Applications

- Photodiode amplifiers ATE
- Instrumentation
- Sensors and controls
- High performance filters Fast precision integrators High performance audio

Pin ConfiguratIons

TOP VIEW(Not to Scale)

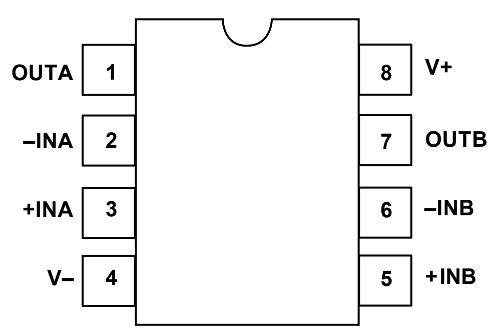

Figure 1. 8-Lead SOIC

Specifications

@ V_S = ±5.0 V, V_{CM} = 0 V, T_A = 25°C, unless otherwise noted.

Table 1.

Parameter	Symbol	Conditions	Min	Typ	Max	Unit
INPUT CHARACTERISTICS						
Offset Voltage	V_{OS}	25°C < T_A < 125°C -40°C < T_A < +125°C		90 150	350 850	µV µV
Input Bias Current	I_B	-40°C < T_A < +85°C -40°C < T_A < +125°C	-10 -250 -2.5	+2 +130 +1.5	+10 +250 +2.5	pA pA nA
Input Offset Current	I_{OS}	 -40°C < T_A < +85°C -40°C < T_A < +125°C	-10 -75 -150	+1 +20 +40	+10 +75 +150	pA pA pA
Input Voltage Range			-2		+3	V
Common-Mode Rejection Ratio	CMRR	V_{CM} = -1.5 V to +2.5 V	90	95		dB
Large SignalVoltage Gain	A_{VO}	RL = 1 kΩ, VO = —3 V to +3 V	100	180		V/mV
Offset Voltage Drift	$\Delta V_{OS}/\Delta T$	-40°C < T_A < +125°C		0.8	3.5	µV/°C
OUTPUT CHARACTERISTICS						
Output Voltage High	V_{OH}	R_L = 1 kΩ, -40°C < T_A < +125°C	3.8	4		V
Output Voltage Low	V_{OL}	R_L = 1 kΩ, -40°C < T_A < +125°C		-4	-3.8	V
Output Current	I_{OUT}	V_{OUT} > ±2 V		±30		mA
POWER SUPPLY						
Power Supply Rejection Ratio Supply Current per Amplifier	PSRR I_{SY}	V_S = ±5 V to ±13 V V_O = 0 V -40°C < T_A < +125°C	100	110 2.5 3.0	 3.0 3.5	dB mA mA
DYNAMIC PERFORMANCE						
Slew Rate	SR	RL = 2 kΩ	40	50		V/µs
Gain Bandwidth Product	GBP			25		MHz
Settling Time	t_S	A_V = +1, 4 V step, to 0.01%		350		ns
NOISE PERFORMANCE						
Voltage Noise	e_n p-p	0.1 Hz to 10 Hz		1.8		µV p-p
Voltage Noise Density	e_n	f = 1 kHz		6		nV/√Hz
Current Noise Density	i_n	f = 1 kHz		5		fA/√Hz
Input Capacitance	C_{IN}					
Differential Mode				8		pF
Common Mode				15		pF
Channel Separation	C_S					
f = 10 kHz				137		dB
f = 300 kHz				120		dB

ELECTRICAL SPECIFICATIONS

@ V_S = ±13 V, V_{CM} = 0 V, T_A = 25°C, unless otherwise noted.

Table 2.

Parameter	Symbol	Conditions	Min	Typ	Max	Unit
INPUT CHARACTERISTICS						
Offset Voltage	V_{OS}	25°C < T_A < 125°C -40°C < T_A < +125°C		90 150	350 850	μV μV
Input Bias Current	I_B	-40°C < T_A < +85°C -40°C < T_A < +125°C	-10 -250 -3.5	+3 +130	+10 +250 +3.5	pA pA nA
Input Offset Current	I_{OS}	 -40°C < T_A < +85°C -40°C < T_A < +125°C	-10 -75 -150	+1.5 +20 +40	+10 +75 +150	pA pA pA
Input Voltage Range			-10.5		+10.5	V
Common-Mode Rejection Ratio	CMRR	V_{CM} = -10 V to +10 V	90	110		dB
Large SignalVoltage Gain	A_{VO}	R_L = 1 kΩ, V_O = -10 V to +10 V	100	200		V/mV
Offset Voltage Drift	$\Delta V_{OS}/\Delta T$	-40°C < T_A < +125°C		0.8	3.5	μV/°C
OUTPUT CHARACTERISTICS						
Output Voltage High	V_{OH}	R_L = 1 kΩ, -40°C < T_A < +125°C	+11.75	+11.84		V
Output Voltage Low	V_{OL}	R_L = 1 kΩ, -40°C < T_A < +125°C		-11.84	-11.75	V
Output Current	I_{OUT}	V_{OUT} > ±10 V		±45		mA
Short-Circuit Current	I_{SC}			±65		
POWER SUPPLY						
Power Supply Rejection Ratio Supply Current per Amplifier	PSRR I_{SY}	V_S = ±5 V to ±13 V V_O = 0 V -40°C < T_A < +125°C	100	110 3.0 3.5	 3.5 4.0	dB mA mA
DYNAMIC PERFORMANCE						
Slew Rate	SR	R_L = 2 kΩ	40	60		V/μs
Gain Bandwidth Product	GBP			25		MHz
Settling Time	t_S	A_V = +1, 10 V step, to 0.01%		600		ns
NOISE PERFORMANCE						
Voltage Noise	e_n p-p	0.1 Hz to 10 Hz		1.8		μV p-p
Voltage Noise Density	e_n	f = 1 kHz		6		nV/√Hz
Current Noise Density	i_n	f = 1 kHz		5		fA/√Hz
Input Capacitance	C_{IN}					
Differential Mode				8		pF
Common Mode				15		pF
Channel Separation	C_S					
f = 10 kHz				137		dB
f = 300 kHz				120		dB

Absolute maximum ratings

Table 3.

Parameter	Rating
Supply Voltage	27.3 V
Input Voltage	VS-to VS+
Differential Input Voltage	±Supply voltage
Output Short-Circuit Duration to GND	Indefinite
Storage Temperature Range	-65°C to +150°C
Operating Temperature Range	-40°C to +125°C
Junction Temperature Range	-65°C to +150°C
Lead Temperature (Soldering, 10 sec)	300°C

Stresses above those listed under Absolute Maximum Ratings may cause permanent damage to the device. This is a stress rating only; functional operation of the device at these or any other conditions above those indicated in the operational section of this specification is not implied. Exposure to absolute maximum rating conditions for extended periods may affect device reliability.

Table 4. Thermal Resistance

Package Type	θ_{JA} [1]	θ_{JC}	Unit
8-Lead SOIC (R)	158	43	°C/W

[1] θ_{JA} is specified for worst-case conditions, that is, θ_{JA} is specified for a device soldered in circuit board for surface-mount packages.

ESD CAUTION

ESD (electrostatic discharge) sensitive device. charged devices and circuit boards can discharge without detection. Although this product features patented or proprietary protection circuitry, damage may occur on devices subjected to high energy ESD. Therefore, proper ESD Precautions should be taken to avoid performance degradation or loss of functionality.

Typical Performance Characteristics

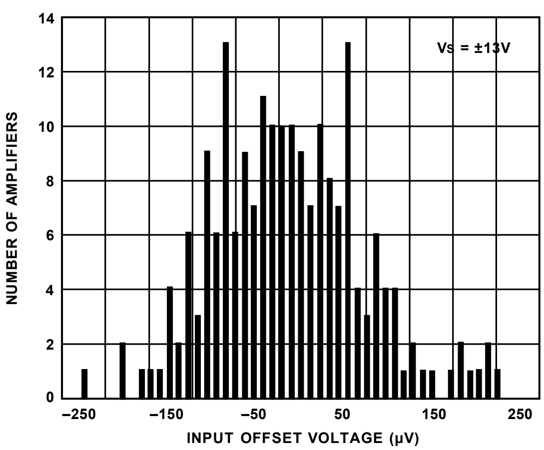

Figure 2. Input Offset Voltage

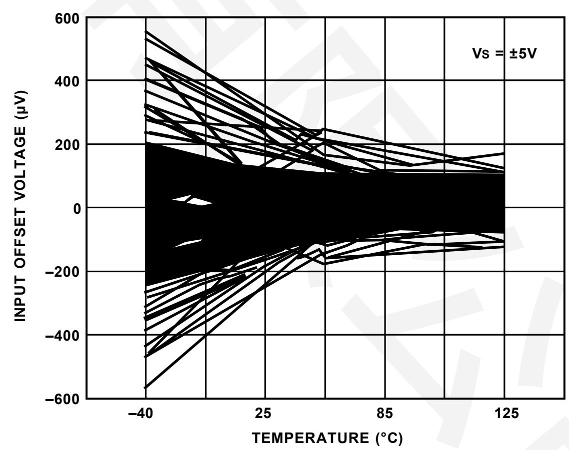

Figure 5. Input Offset Voltage vs. Temperature at ±5 V (300 Amplifiers)

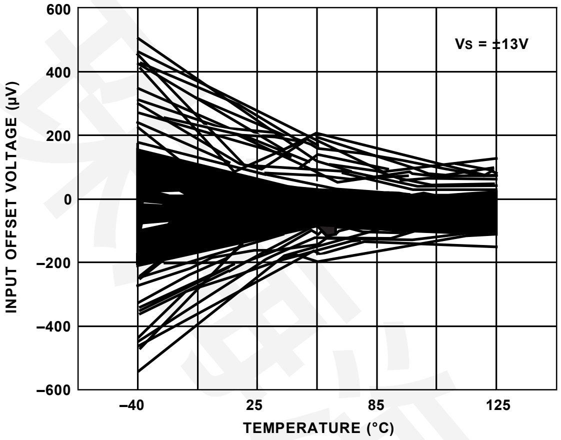

Figure 3. Input Offset Voltage vs. Temperature at ±13 V (300 Amplifiers)

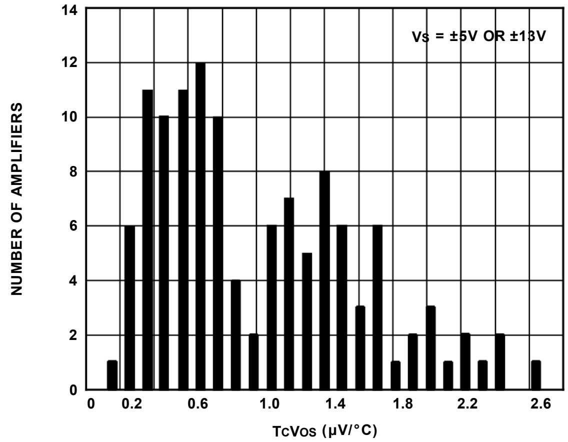

Figure 6. Input Offset Voltage Drift

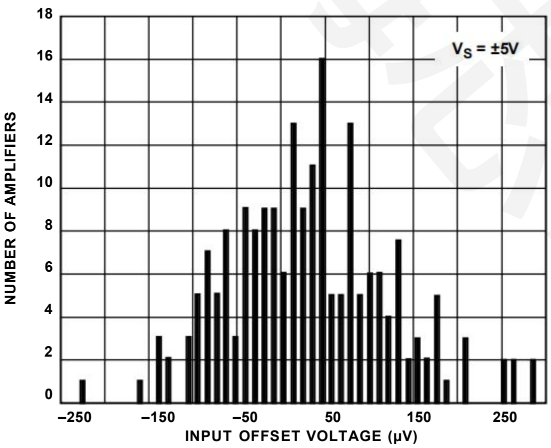

Figure 4. Input Offset Voltage

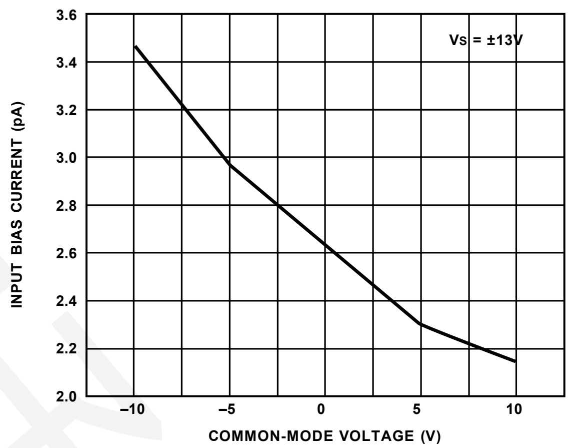

Figure 7. Input Bias Current vs. Common-Mode Voltage

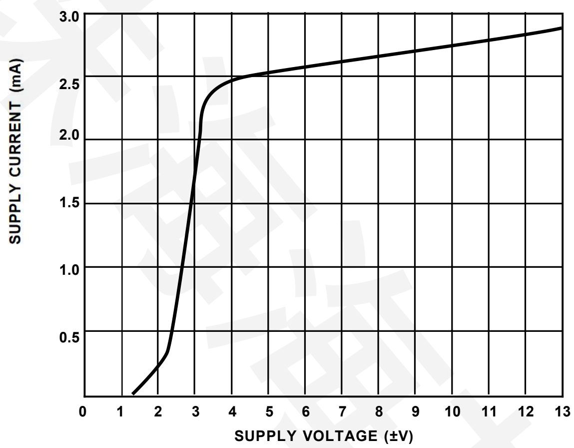

Figure 8. Supply Current vs. Supply Voltage

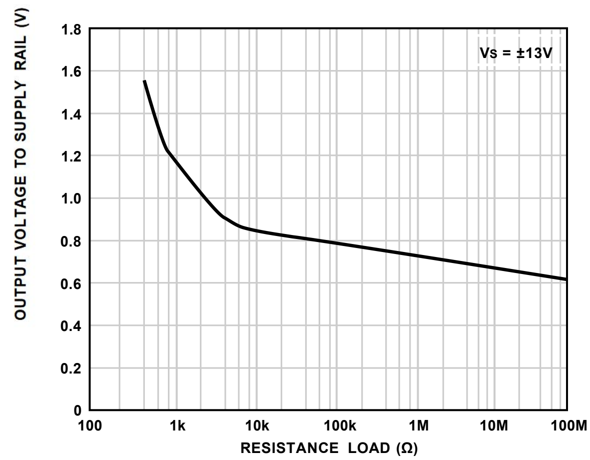

Figure 11. Output Voltage to Supply Rail vs. Resistance Load

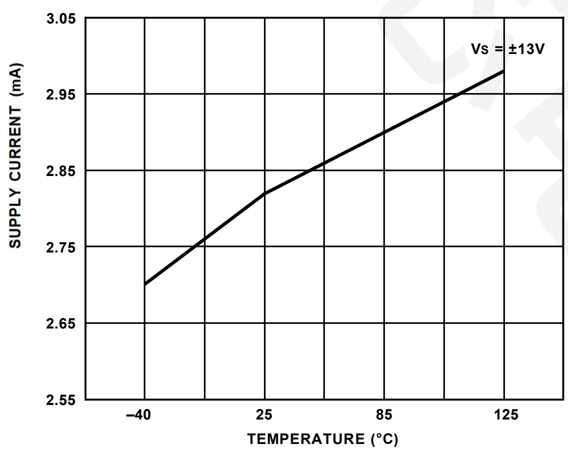

Figure 9. Supply Current vs. Temperature

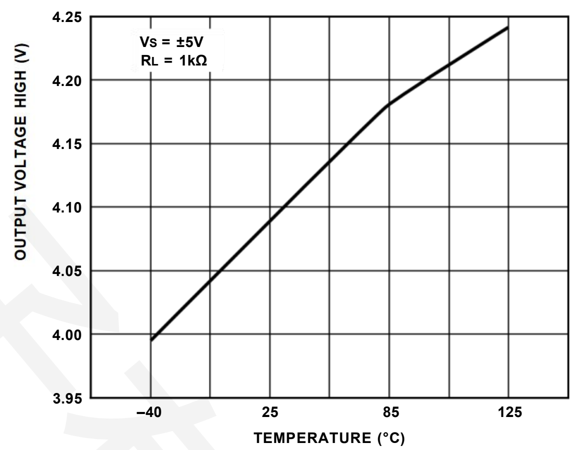

Figure 12. Output Voltage High vs. Temperature

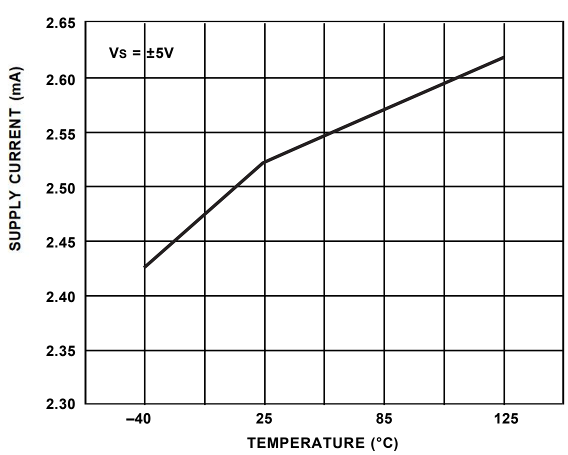

Figure 10. Supply Current vs. Temperature

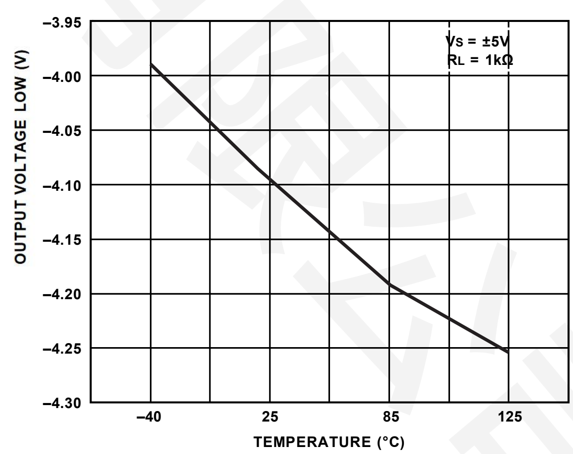

Figure 13. Output Voltage Low vs. Temperature

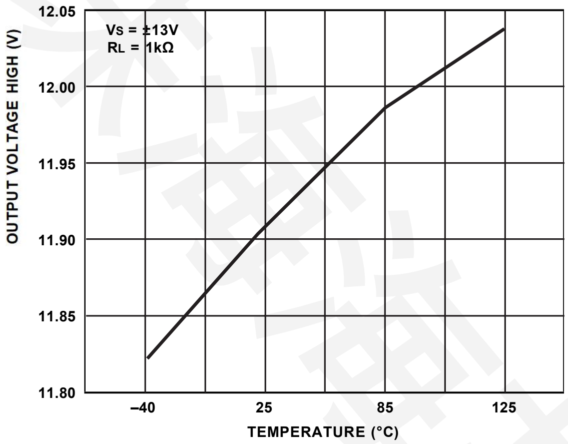

–11.80

Figure 14. Output Voltage High vs. Temperature

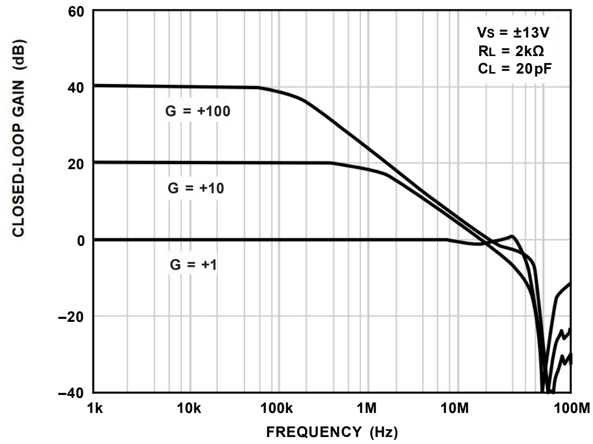

Figure 17. Closed-Loop Gain vs. Frequency

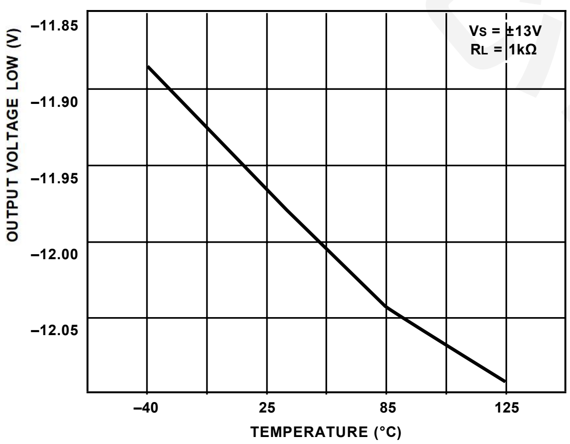

Figure 15. Output Voltage Low vs. Temperature

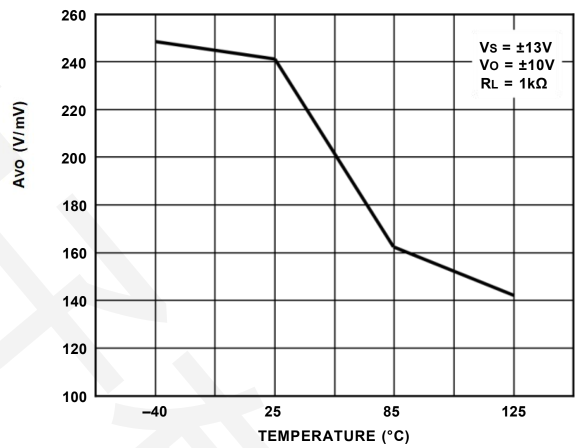

Figure 18. Avo vs. Temperature

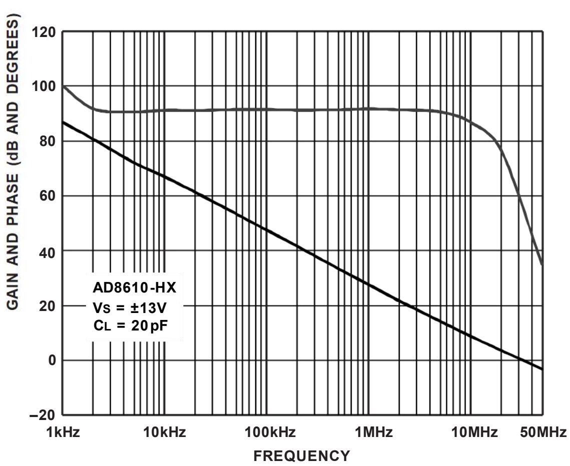

Figure 16. Open-Loop Gain and Phase vs. Frequency

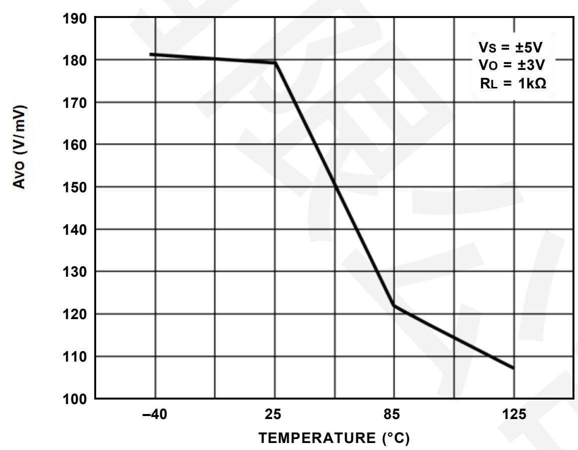

Figure 19. Avo vs. Temperature

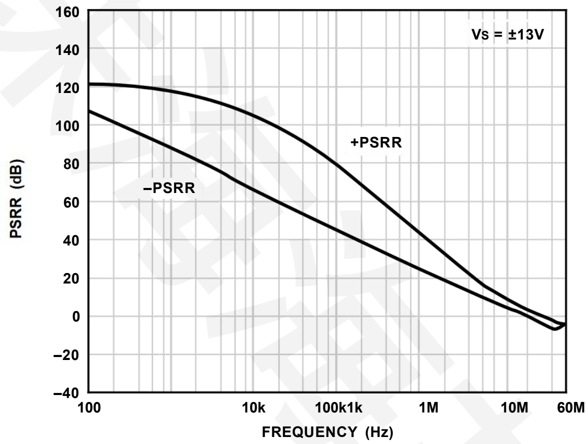

Figure 20. PSRR vs. Frequency

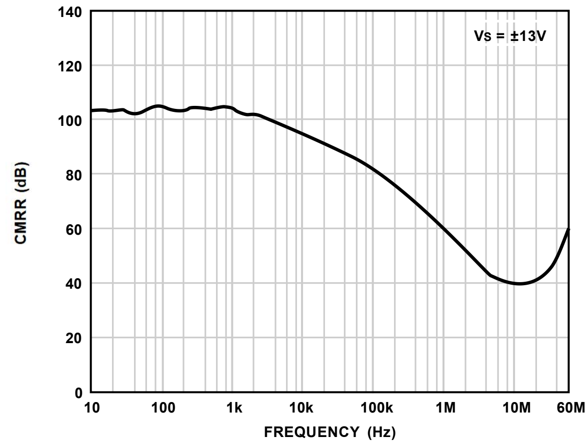

Figure 23. CMRR vs. Frequency

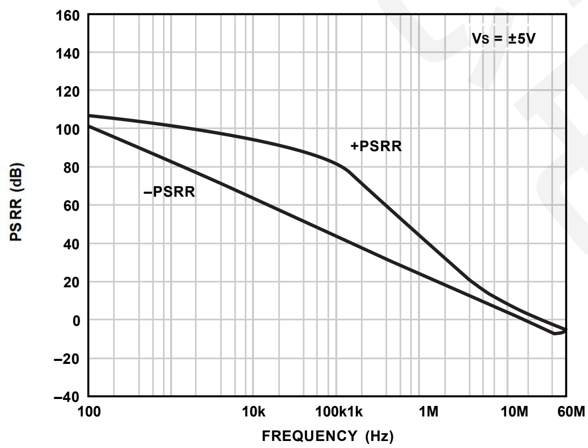

Figure 21. PSRR vs. Frequency

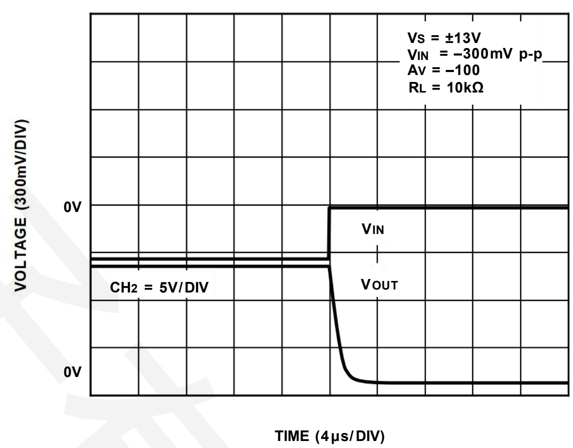

Figure 24. Positive Overvoltage Recovery

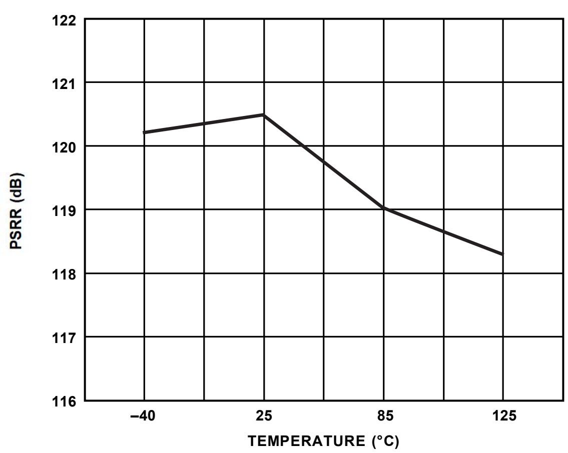

Figure 22. PSRR vs. Temperature

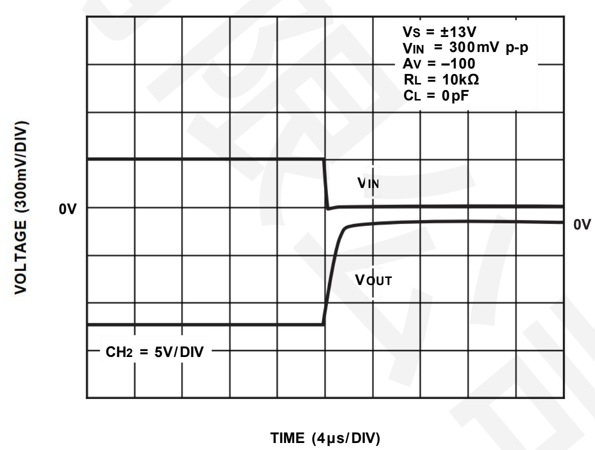

Figure 25. Negative Overvoltage Recovery

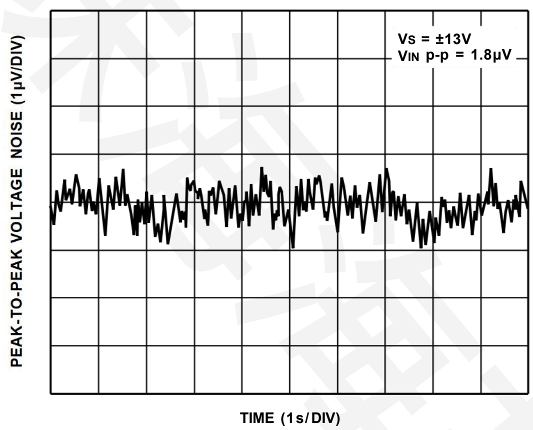

Figure 26. 0.1 Hz to 10 Hz Input Voltage Noise

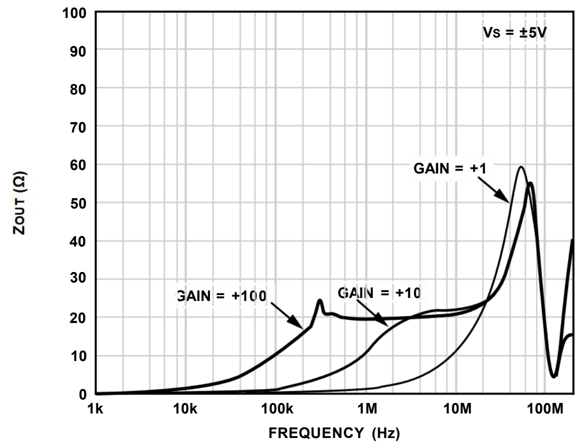

Figure 29. ZOUT vs. Frequency

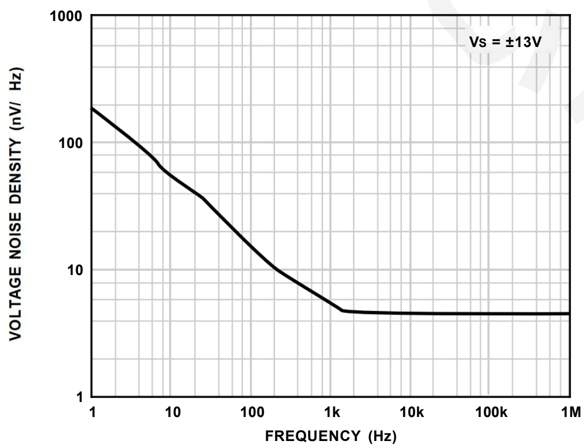

Figure 27. Input Voltage Noise Density vs. Frequency

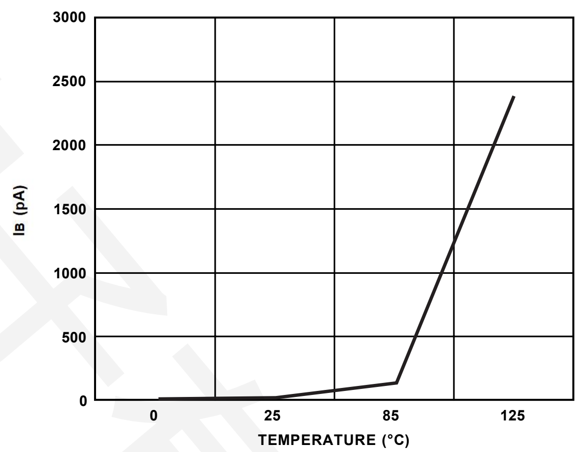

Figure 30. Input Bias Current vs. Temperature

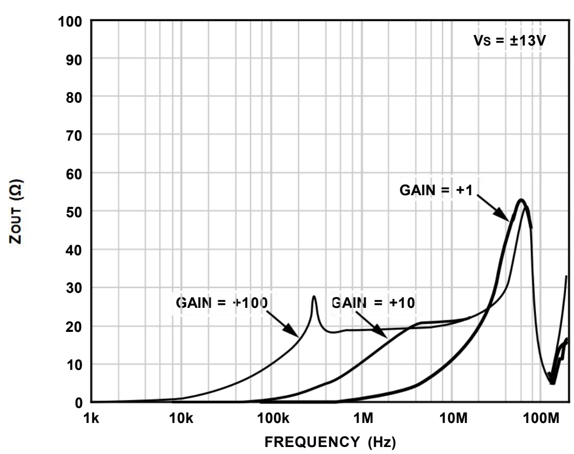

Figure 28. ZOUT vs. Frequency

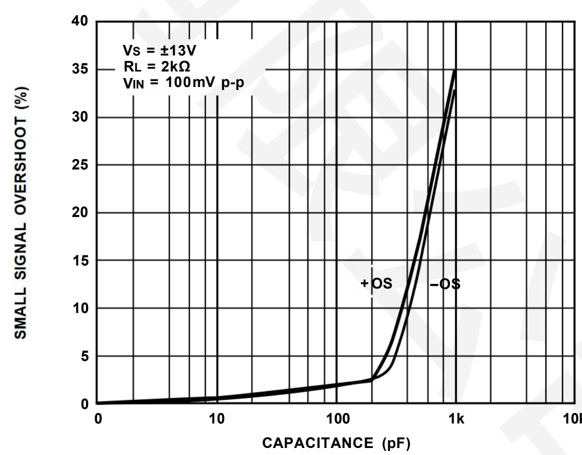

Figure 31. Small Signal Overshoot vs. Load Capacitance

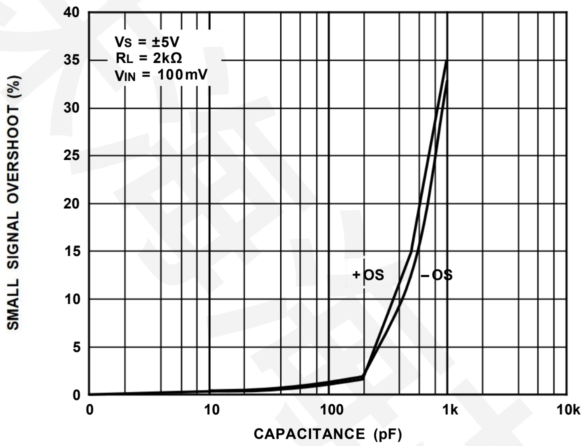

Figure 32. Small Signal Overshoot vs. Load Capacitance

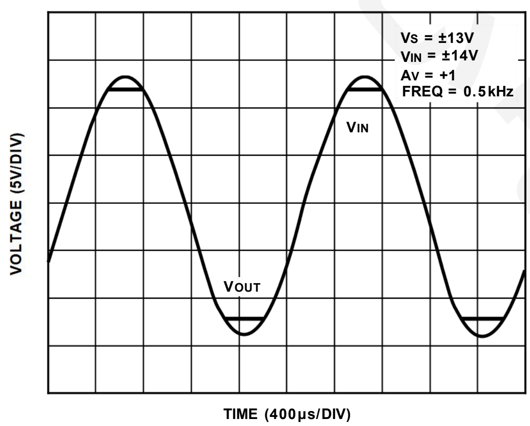

Figure 33. No Phase Reversal

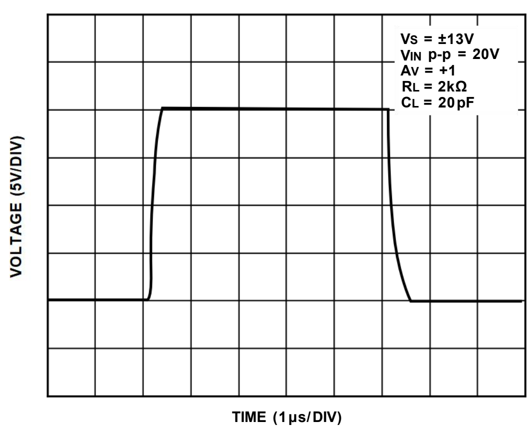

Figure 34. Large Signal Response at G = +1

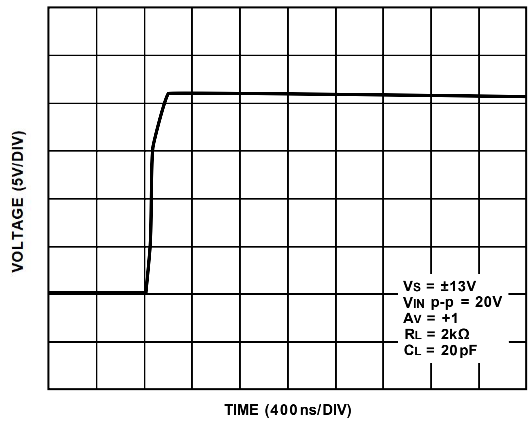

Figure 35. +Slew Rate at G = +1

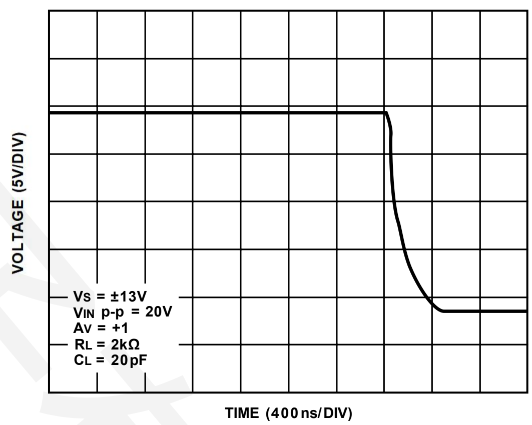

Figure 36. –Slew Rate at G = +1

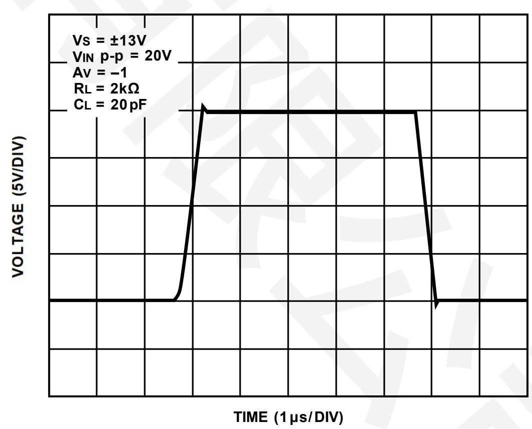

Figure 37. Large Signal Response at G = –1

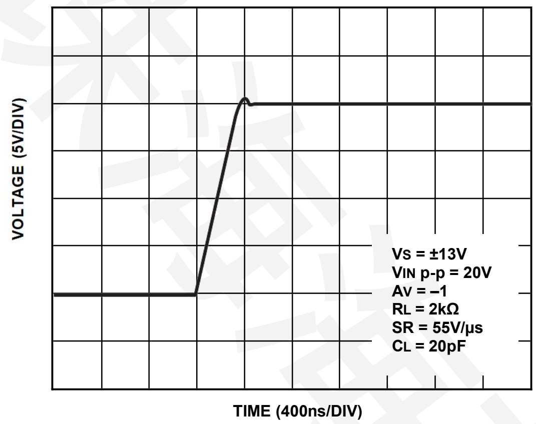

Figure 39. +Slew Rate at G = −1

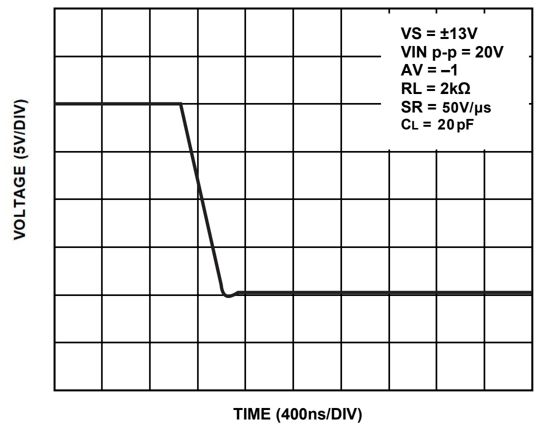

Figure 40. –Slew Rate at G = −1

Theory of operation

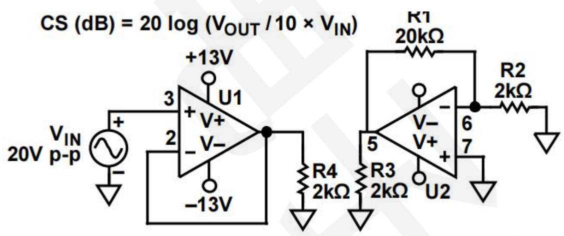

FUNCTIONAL DESCRIPTION

The AD8620ARZ-HX XFCB is fully dielectrically isolated (DI) and used in conjunction with N-channel JFET technology and thin film resistors (that can be trimmed) to create the JFET input amplifier. Dielectrically isolated NPN and PNP transistors fabricated on XFCB have an f_T > 3 GHz. Low TC thin film resistors enable very accurate offset voltage and offset voltage temperature coefficient trimming. The AD8620ARZ-HX is unconditionally stable in all gains,
even with capacitive loads well in excess of 1 nF. The AD8610-HX is offered in the tiny 8-lead MSOP as well as narrow 8-lead SOIC surface-mount packages and is fully specified with supply voltages from ±5.0 V to ±13 V. The very wide specified temperature range, up to 125°C, guarantees superior operation in systems with little or no active cooling.
The unique input architecture ofthe AD8620ARZ-HX features extremely low input bias currents and very low input offset voltage. Low power consumption minimizes the die temperature and maintains the very low input bias current. Unlike many competi- tive JFET amplifiers, the AD8620ARZ-HX input bias currents are low even at elevated temperatures. Typical bias currents are less than 200 pA at 85°C. The gate current of a JFET doubles every 10°C, resulting in a similar increase in input bias current over temperature. Give special care to the PC board layout to minimize leakage currents between PCB traces. Improper layout and board handling generates a leakage current that exceeds the bias current ofthe AD8620ARZ-HX.

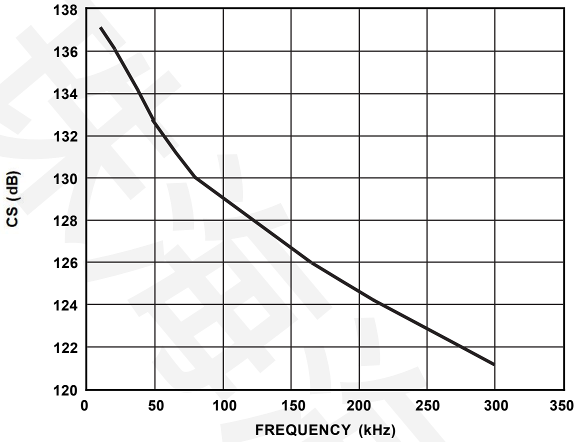

Figure 41. AD8620ARZ-HX Channel Separation Graph

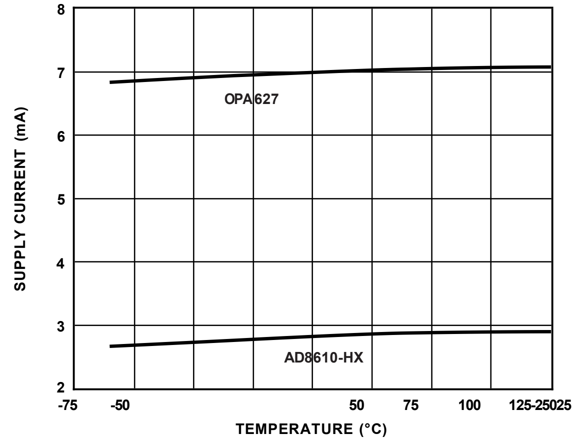

Figure 42. Supply Current vs. Temperature

Power Consumption

A major advantage ofthe AD8620ARZ-HX in new designs is the power saving capability. Lower power consumption of the AD8620ARZ-HX makes them much more attractive for portable instrumentation and for high density systems, simplifying thermal management, and reducing power-supply performance require- ments. Compare the power consumption ofthe AD8610-HX vs. the OPA627 in Figure 42.

Driving Large Capacitive Loads

The AD8620ARZ-HX have excellent capacitive load driving capability and can safely drive up to 10 nF when operating with a ±5.0 V supply. Figure 43 and Figure 44 compare the AD8620ARZ-HX against the OPA627 in the noninverting gain configu- ration driving a 10 kΩ resistor and 10,000 pF capacitor placed in parallel on its output, with a square wave input set to a frequency of 200 kHz. The AD8620ARZ-HX have much less ringing than the OPA627 with heavy capacitive loads.

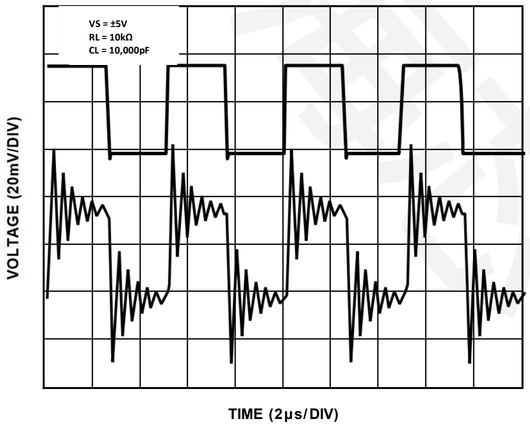

Figure 43. OPA627 Driving C_L = 10,000 pF

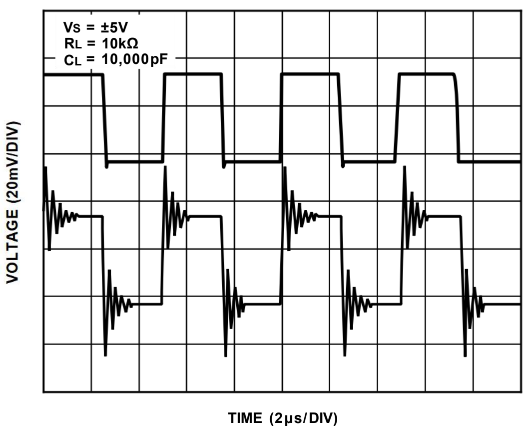

Figure 44. AD8620ARZ-HX Driving C_L = 10,000 pF

The AD8620ARZ-HX can drive much larger capacitances without any external compensation. Although the AD8620ARZ -HX are stable with very large capacitive loads, remember that this capacitive loading limits the bandwidth of the amplifier. Heavy capacitive loads also increase the amount of overshoot and ringing at the output. Figure 46 and Figure 47 show the AD8620ARZ-HX and the OPA627 in a noninverting gain of +2 driving 2 μF of capacitance load. The ringing on the OPA627 is much larger in magnitude and continues 10 times longer than the AD8620ARZ-HX.

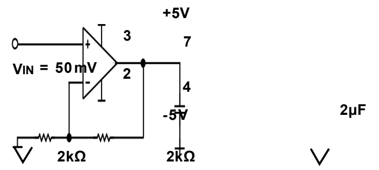

Figure 45. Capacitive Load Drive Test Circuit

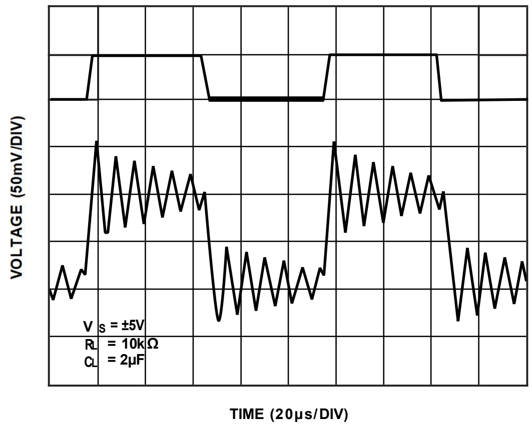

Figure 46. OPA627 Capacitive Load Drive, A_V = +2

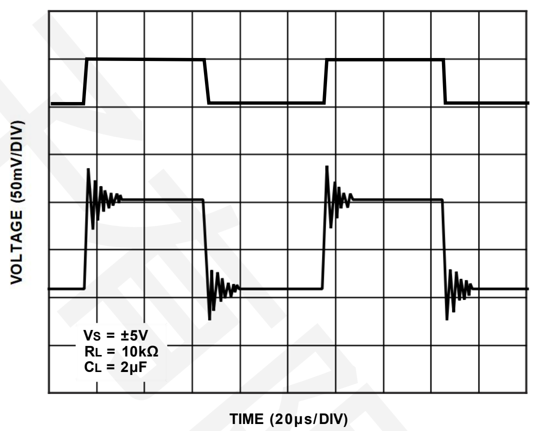

Figure 47. AD8620ARZ-HX Capacitive Load Drive, A_V = +2

Slew Rate (Unity Gain Inverting vs. Noninverting)

Amplifiers generally have a faster slew rate in an inverting unity gain configuration due to the absence of the differential input capacitance. Figure 48 through Figure 51 show the performance ofthe AD8620ARZ-HX configured in a unity gain of –1 compared to the OPA627. The AD8620ARZ-HX slew rate is more symmetrical, and both the positive and negative transitions are much cleaner than in the OPA627.

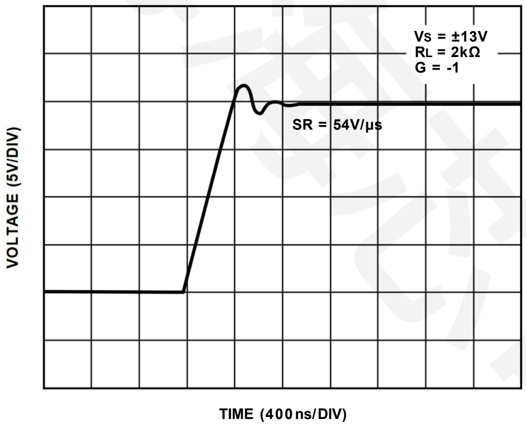

Figure 48. +Slew Rate of AD8620ARZ-HX in Unity Gain of –1

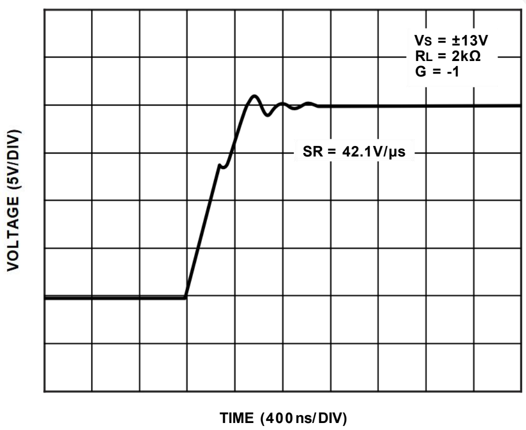

Figure 49. +Slew Rate of OPA627 in Unity Gain of –1

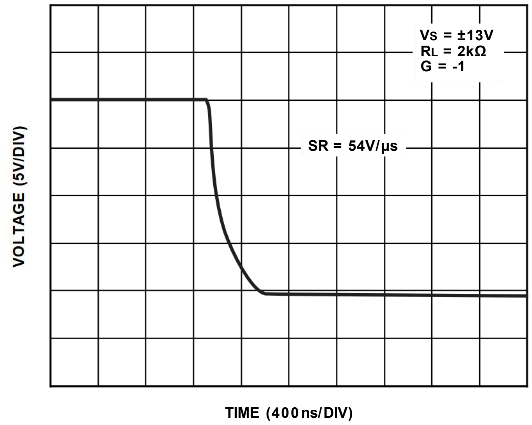

Figure 50. –Slew Rate of AD8620ARZ-HX in Unity Gain of –1

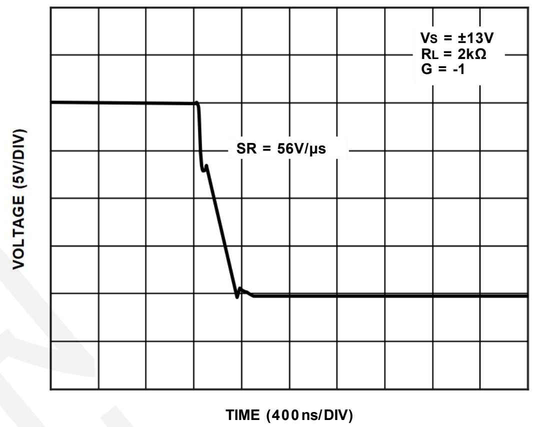

Figure 51. –Slew Rate of OPA627 in Unity Gain of –1

The AD8620ARZ-HX have a very fast slew rate of 60 V/µs even when configured in a noninverting gain of +1. This is the toughest condition to impose on any amplifier because the input common-mode capacitance of the amplifier generally makes its SR appear worse. The slew rate of an amplifier varies according to the voltage difference between its two inputs. To observe the maximum SR, a voltage difference of about 2 V between the inputs must be ensured. This is required for virtually any JFET op amp so that one side of the op amp input circuit is completely off, thus maximizing the current available to charge and discharge the internal compensation capacitance. Lower differential drive voltages produce lower slew rate readings. A JFET input op amp with a slew rate of 60 V/µs at unity gain with V_{IN} = 10 V may slew at 20 V/µs if it is operated at a gain of +100 with V_{IN} = 100 mV.

The slew rate ofthe AD8620ARZ-HX is double that of the OPA627 when configured in a unity gain of +1 (see Figure 52 and Figure 53).

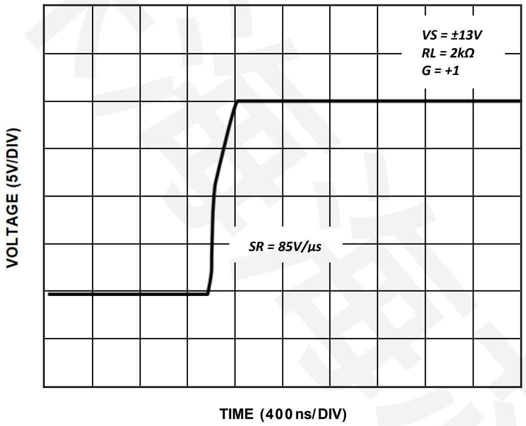

Figure 52. +Slew Rate of AD8620ARZ-HX in Unity Gain of +1

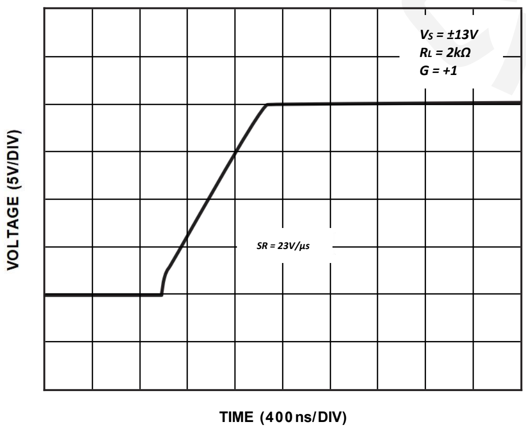

Figure 53. +Slew Rate of OPA627 in Unity Gain of +1

The slew rate of an amplifier determines the maximum frequency at which it can respond to a large signal input. This frequency (known as full power bandwidth or FPBW) can be calculated for a given distortion (for example, 1%) from the equation

$$FPBW = \frac{SR}{\left(2\pi \times V_{PEAK}\right)}$$

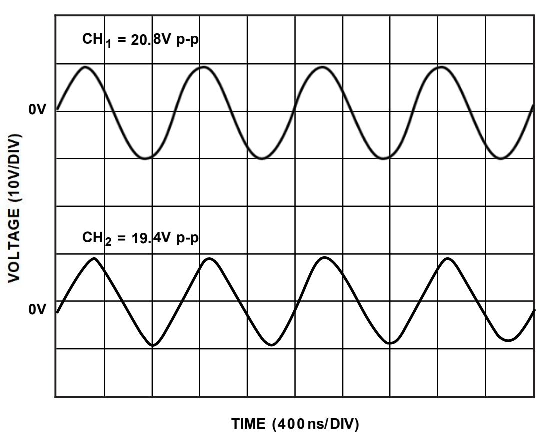

Figure 54. AD8610-HX FPBW

Input Overvoltage Protection

When the input of an amplifier is driven below V_{EE} or above V_{CC} by more than one V_{BE}, large currents flow from the substrate through the negative supply (V−) or the positive supply (V+), respectively, to the input pins and can destroy the device. If the input source can deliver larger currents than the maximum forward current of the diode (>5 mA), a series resistor can be added to protect the inputs. With its very low input bias and offset current, a large series resistor can be placed in front of the AD8620ARZ-HX inputs to limit current to below damaging levels. Series resistance of 10 kΩ generates less than 25 µV of offset. This 10 kΩ allows input voltages more than 5 V beyond either power supply. Thermal noise generated by the resistor adds 7.5 nV/√Hz to the noise ofthe AD8620ARZ-HX. Forthe AD8620ARZ-HX, differential voltages equal to the supply voltage do not cause any problems (see Figure 54). In this context, note that the high breakdown voltage of the input FETs eliminates the need to include clamp diodes between the inputs ofthe amplifier, a practice that is mandatory on many precision op amps. Unfortunately,clamp diodes greatly interfere with many application circuits, such as precision rectifiers and comparators. The AD8620ARZ-HX is free from these limitations.

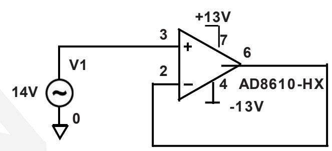

Figure 55. Unity Gain Follower

No Phase Reversal

Many amplifiers misbehave when one or both of the inputs are forced beyond the input common-mode voltage range. Phase reversal is typified by the transfer function of the amplifier, effectively reversing its transfer polarity. In some cases, this can cause lockup and even equipment damage in servo systems and can cause permanent damage or no recoverable parameter shifts to the amplifier itself. Many amplifiers feature compensation circuitry to combat these effects, but some are only effective for the inverting input. The AD8620ARZ-HX are designed to prevent phase reversal when one or both inputs are forced beyond their input common-mode voltage range.

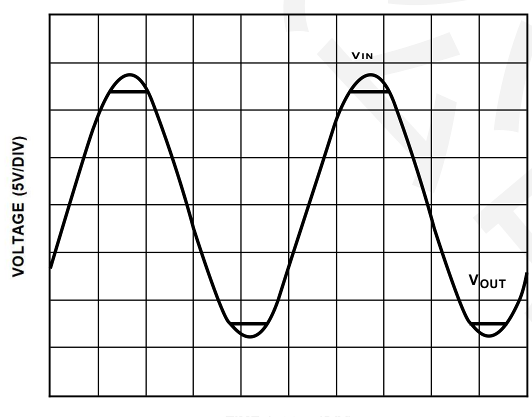

Figure 56. No Phase Reversal

THD Readings vs. Common-Mode Voltage

Total harmonic distortion ofthe AD8620ARZ-HX is well below 0.0006% with any load down to 600 Ω . The AD8610-HX outperforms the OPA627 for distortion, especially at frequencies above 20 kHz.

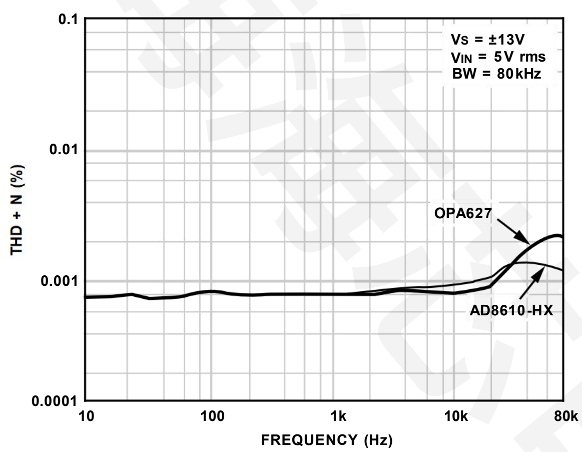

Figure 57. AD8610-HX vs. OPA627 THD + Noise @ V_{CM} = 0 V

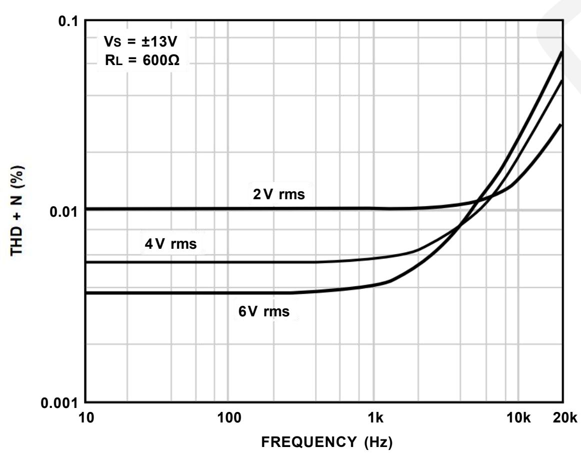

Figure 58. THD + Noise vs. Frequency

Noise vs. Common-Mode Voltage

The AD8620ARZ-HX noise density varies only 10% over the input range, as shown inTable5.

Table 5. Noise vs. Common-Mode Voltage

V_{CM} at f = 1 kHz (V)	Noise Reading (nV/√Hz)
−10	7.21
−5	6.89
0	6.73
+5	6.41
+10	7.21

Settling Time

The AD8620ARZ-HX have a very fast settling time, even to a very tight error band, as can be seen from Figure 59. The AD8620ARZ-HX is configured in an inverting gain of +1 with 2 kΩ input and feedback resistors. The output is monitored with a 10×,10 MΩ, 11.2 pF scope probe.

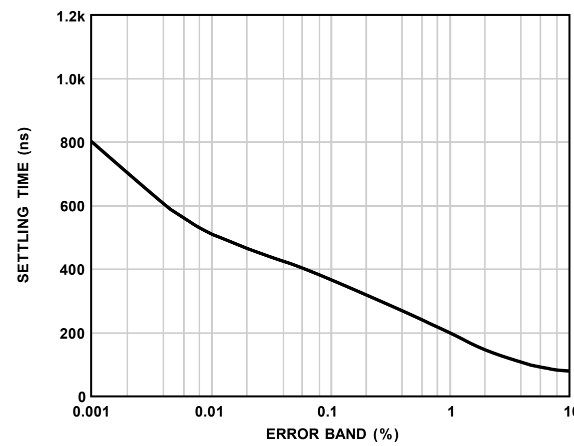

Figure 59. AD8620ARZ-HX Settling Time vs. Error Band

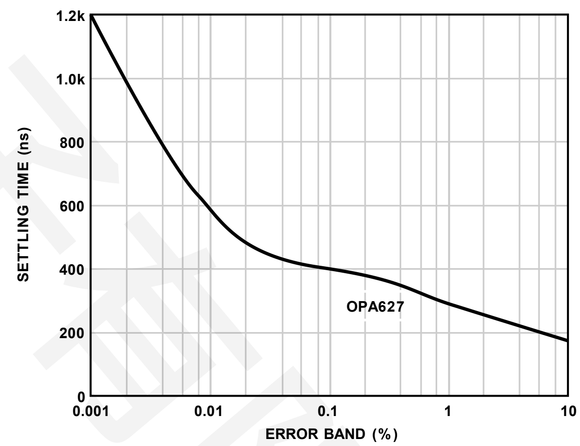

Figure 60. OPA627 Settling Time vs. Error Band

The AD8620ARZ-HX maintain this fast settling time when loaded with large capacitive loads, as shown in Figure 61.

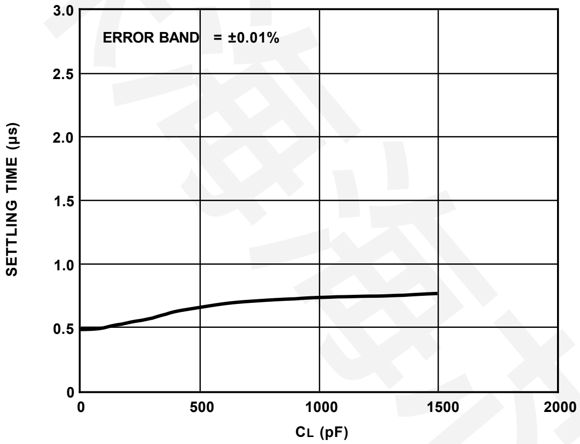

Figure 61. AD8620ARZ-HX Settling Time vs. Load Capacitance

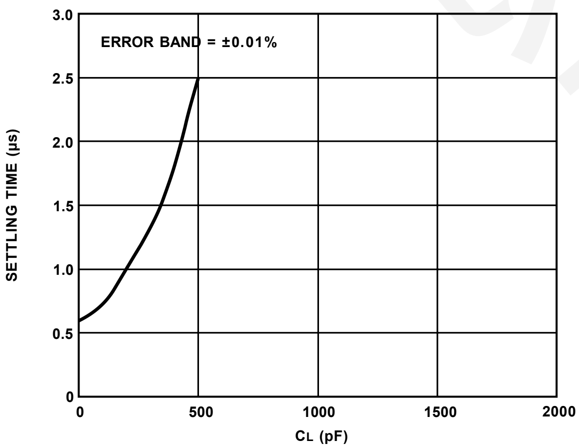

Figure 62. OPA627 Settling Time vs. Load Capacitance

Output Current Capability

The AD8620ARZ-HX can drive very heavy loads due to its high output current. It is capable of sourcing or sinking 45 mA at ±10 V output. The short-circuit current is quite high and the part is capable of sinking about 95 mA and sourcing over 60 mA while operating with supplies of ±13 V. Figure 63 and Figure 64 compare the output voltage vs. load current of AD8620ARZ-HX and OPA627.

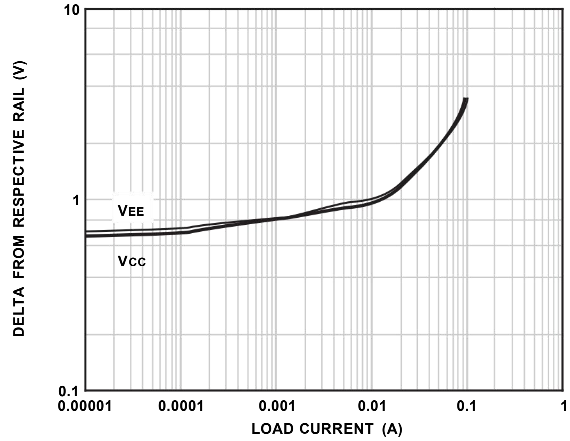

Figure 63. AD8620ARZ-HX Dropout from ±13 V vs. Load Current

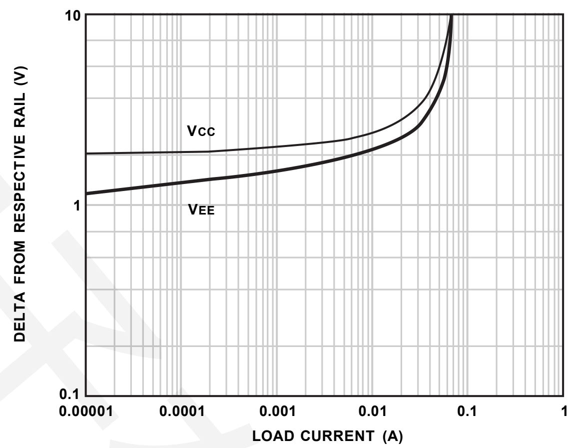

Figure 64. OPA627 Dropout from ±15 V vs. Load Current

Although operating conditions imposed on the AD8620ARZ-HX (±13 V) are less favorable than the OPA627 (±15 V), it can be seen that the AD8620ARZ-HX have much better drive capability (lower headroom to the supply) for a given load current.

Operating with Supplies Greater than ±13 V

The AD8620ARZ-HX maximum operating voltage is specified at ±13 V. When ±13 V is not readily available, an inexpensive LDO can provide ±12 V from a nominal ±15 V supply.

Input Offset Voltage Adjustment

Offset of AD8610-HX is very small and normally does not require additional offset adjustment. However, the offset adjust pins can be used as shown in Figure 66 to further reduce the dc offset. By using resistors in the range of 50 kΩ, offset trim range is ±3.3 mV.

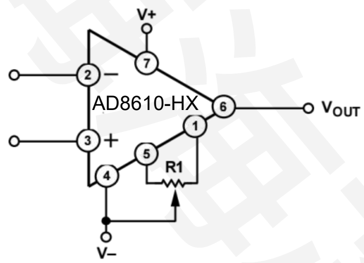

Figure 65. Offset Voltage Nulling Circuit

Programmable Gain Amplifier (PGA)

The combination of low noise, low input bias current, low input offset voltage, and low temperature drift make the AD8620ARZ-HX a perfect solution for programmable gain amplifiers. PGAs are often used immediately after sensors to increase the dynamic range of the measurement circuit. Historically, the large on resistance of switches (combined with the large I_B currents of amplifiers) created a large dc offset in PGAs. Recent and improved monolithic switches and amplifiers completely remove these problems. A PGA discrete circuit is shown in Figure 67. In Figure 67, when the 10 pA bias current of the AD8610-HX is dropped across the (<5 Ω) R_{ON} of the switch, it results in a negligible offset error.

When high precision resistors are used, as in the circuit of Figure 67, the error introduced by the PGA is within the ½ LSB requirement for a 16-bit system.

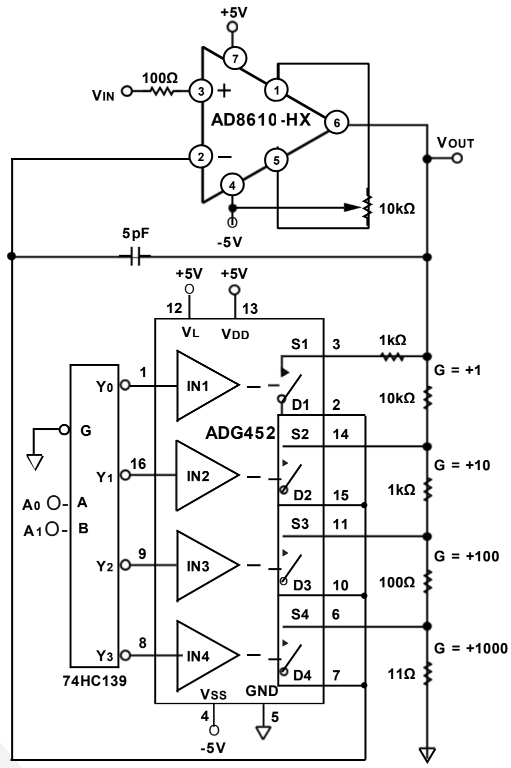

Figure 66. High Precision PGA

1. Room temperature error calculation due to R_{ON} and I_B

   $\Delta V_{OS} = I_B \times R_{ON} = 2\ \text{pA} \times 5\ \Omega = 10\ \text{pV}$

   Total Offset = AD8610-HX (*Offset*) + ΔV_{OS}

   Total Offset = AD8610-HX (*Offset_ Trimmed*) +

   ΔV_{OS} *Total Offset* = 5 μV + 10 pV ≈ 5 μV

2. Full temperature error calculation due to R_{ON} and I_B

   ΔV_{OS} (@ 85°C) = I_B (@ 85°C) × R_{ON} (@ 85°C) =
   250 pA × 15 Ω = 3.75 nV

3. The temperature coefficient of switch and AD8620ARZ-HX combined is essentially the same as the T_CV_{OS} of the AD8620ARZ-HX.

   $\Delta V_{OS}/\Delta T(total) = \Delta V_{OS}/\Delta T$(AD8620ARZ-HX) +
   $\Delta V_{OS}/\Delta T(I_B \times R_{ON})$

   $\Delta V_{OS}/\Delta T(total)$ = *0.5* μV/°C + 0.06 nV/°C ≈ 0.5 μV/°C

High Speed Instrumentation Amplifier

The 3-op-amp instrumentation amplifiers shown in Figure 68 can provide a range of gains from unity up to 1000 or higher. The instrumentation amplifier configuration features high common-mode rejection, balanced differential inputs, and stable, accurately defined gain. Low input bias currents and fast settling are achieved with the JFET input AD8620ARZ-HX. Most instrumentation amplifiers cannot match the high frequency performance of this circuit. The circuit bandwidth is 25 MHz at a gain of 1, and close to 5 MHz at a gain of 10. Settling time for the entire circuit is 550 ns to 0.01% for a 10 V step (gain = 10). Note that the resistors around the input pins need to be small enough in value so that the RC time constant they form in combination with stray circuit capacitance does not reduce circuit bandwidth.

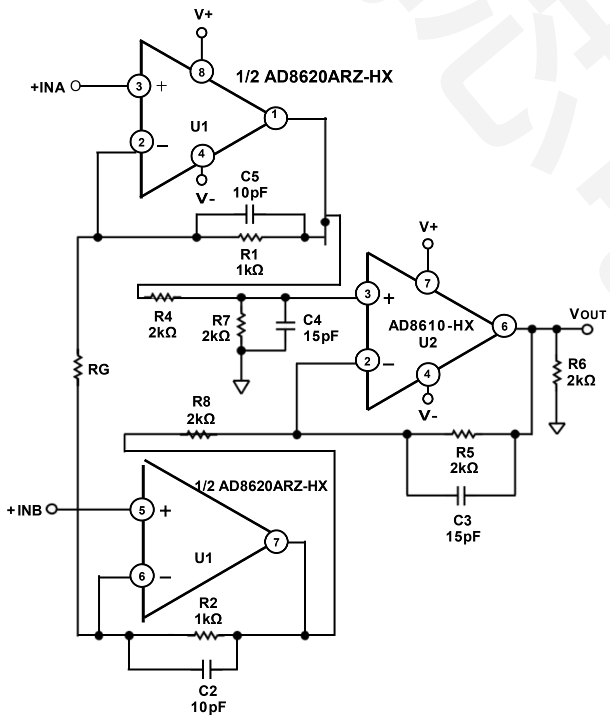

Figure 67. High Speed Instrumentation Amplifier

High Speed Filters

The four most popular configurations are Butterworth, Elliptical, Bessel (Thompson), and Chebyshev. Each type has a response that is optimized for a given characteristic, as shown in Table6.

In active filter applications using operational amplifiers, the dc accuracy of the amplifier is critical to optimal filter performance. The offset voltage and bias current of the amplifier contribute to output error. Input offset voltage is passed by the filter and can be amplified to produce excessive output offset. For low frequency applications requiring large value input resistors, bias and offset currents flowing through these resistors also generate an offset voltage.

At higher frequencies, the dynamic response of the amplifier must be carefully considered. In this case, slew rate, bandwidth, and open-loop gain play a major role in amplifier selection. The slew rate must be both fast and symmetrical to minimize distortion. The bandwidth of the amplifier, in conjunction with the gain of the filter, dictates the frequency response of the filter. The use of high performance amplifiers, such as the AD8620ARZ-HX, minimizes both dc and ac errors in all active filter applications.

Second-Order, Low-Pass Filter

Figure 69shows the AD8610-HX configured as a second-order, Butterworth, low-pass filter. With the values as shown, the
design corner was 1 MHz, and the bench measurement was 974 kHz. The wide bandwidth ofthe AD8620ARZ-HX allows corner frequencies into the megahertz range, but the input capacitances should be taken into account by making C1 and C2 smaller than the calculated values. The following equations can be used for component selection:

R1 = *R2* = *User Selected* (Typical Values = 10 kΩ to 100 kΩ)

$$C1 = \frac{1.414}{(2\pi)(f_{CUTOFF})(R1)}$$

$$C2 = \frac{0.707}{(2\pi)(f_{CUTOFF})(R1)}$$

where *C1* and *C2* are in farads.

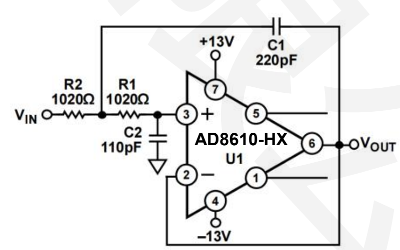

Figure 68. Second-Order, Low-Pass Filter

Table 6. Filter Types

Type	Sensitivity	Overshoot	Phase	Amplitude (Pass Band)
Butterworth	Moderate	Good		Maximum flat
Chebyshev	Good	Moderate	Nonlinear	Equal ripple
Elliptical	Best	Poor		Equal ripple
Bessel (Thompson)	Poor	Best	Linear	

High Speed, Low Noise Differential Driver

The AD8620ARZ-HX is a perfect candidate as a low noise differential driver for many popular ADCs. There are also other applications (such as balanced lines) that require differential drivers.

The circuit of Figure 70 is a unique line driver widely used in industrial applications. With ±13 V supplies, the line driver can deliver a differential signal of 23 V p-p into a 1 kΩ load. The high slew rate and wide bandwidth ofthe AD8620ARZ-HX combine to yield a full power bandwidth of 145 kHz while the low noise front end produces a referred-to-input noise voltage spectral density of 6 nV/√Hz. The design is a balanced transmission system without transformers, where output common-mode rejection of noise is of paramount importance. Like the transformer-based design, either output can be shorted to ground for unbalanced line driver applications without changing the circuit gain of 1. This allows the design to be easily set to noninverting, inverting, or differential operation.

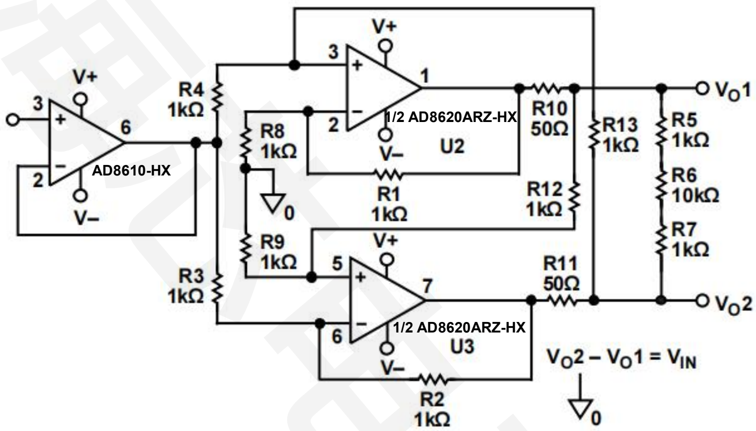

Figure 69. Differential Driver

Outline dimensions

SOIC8